Geochronological Results from Reconnaissance Investigations in the Beetle Infested Zone, South-Central British Columbia

by M.G. Mihalynuk, R.M. Friedman[1] and T.D. Ullrich[1]

KEYWORDS: geochronology, isotopic age, uranium-lead zircon, $^{40}Ar/^{39}Ar$, mineral potential, mountain pine beetle, economic diversification, Stikine Terrane, Cache Creek Terrane

INTRODUCTION

Forestry is the principal economic engine for many communities within the interior of British Columbia. Infestations of mountain pine beetle have affected most forests in this part of the province (Fig 1) and, as a result of widespread pine tree mortality, a downturn within the forestry sector is anticipated. The BC government is working to stimulate economic diversification within the Beetle Infested Zone (BIZ) to soften these negative economic impacts.

Mineral exploration and mineral resource development within the BIZ have lagged behind other prospective parts of the province (Mihalynuk, 2007a). Low levels of historical exploration mean more opportunity for future mineral discoveries and, as such, these industries could bring economic diversification to the BIZ. To help the mineral exploration industry justify investments in the BIZ, the BC Geological Survey has refocused most of its field programs into the area (*see* 'Foreword', page iii). We report here on geochronological data arising from a 2006 reconnaissance field program that investigated methods to enhance the efficacy of geological fieldwork within the BIZ (e.g., Mihalynuk, 2007b; Mihalynuk et al., 2008).

LOCATION

Data reported here are from samples collected in three widespread areas within the BIZ — east of southern Babine Lake, near Riske Creek and west of the Iron Mask batholith (Fig 1).

Samples were collected from three sites east of southern Babine Lake — two sites are along the main logging haul road (named 'Phantom Road') between 4 and 6 km northwest of Boling Point on Babine Lake (samples MMI06-7-12 and MMI06-24-4, Table 1), and the third site is a recently active borrow pit approximately 1 km southwest of Cunningham Lake (sample MMI06-5-1, Table 1).

[1] *Pacific Centre for Isotopic and Geochemical Research, The University of British Columbia, Vancouver, BC*

This publication is also available, free of charge, as colour digital files in Adobe Acrobat® PDF format from the BC Ministry of Energy, Mines and Petroleum Resources website at http://www.em.gov.bc.ca/Mining/Geolsurv/Publications/catalog/cat_fldwk.htm

All three sites are within an area most recently mapped at 1:100 000 scale by MacIntyre and Schiarizza (1999).

Samples from the Riske Creek area were collected from a site 27 km southwest of Williams Lake, located between Cotton Road and the village of Toosey (sample MMI06-34-8, Table 1). This area has been most recently mapped at 1:50 000 scale by Mihalynuk and Harker (2007; *see also* Mihalynuk et al., 2007), who included the sample location and age (without data) on their map.

Sample collection in the Iron Mask batholith area was from west of the batholith, approximately 2 km south of Jacko Lake and 15 km southwest of Kamloops (sample MMI04-11-7b, Table 1). A recent regional mapping and data compilation that covered this area (Logan and Mihalynuk, 2006) included the sample site within the 'Cherry Creek tectonic zone'.

METHODS

All sample preparation and analytical work for the U-Pb and $^{40}Ar/^{39}Ar$ isotopic ages presented here was conducted at the Pacific Centre for Isotopic and Geochemical Research (PCIGR) at the Department of Earth and Ocean Sciences, The University of British Columbia.

The U-Pb isotopic age determinations reported here were by Thermal Ionization Mass Spectroscopy (U-Pb TIMS). The $^{40}Ar/^{39}Ar$ isotopic age determinations were by the laser-induced step-heating technique. Details of the both analytical techniques are presented in Logan et al. (2007).

ISOTOPIC AGE DETERMINATIONS

A synoptic description of the sample set and geochronological results are presented in Table 1. Results of U-Pb isotopic analyses are reported in Table 2, and summary data for $^{40}Ar/^{39}Ar$ plots are reported in Table 3. Complete digital data sets are available in Ullrich et al. (2008).

Uranium-lead analyses were performed on zircons recovered from samples MMI06-5-1 and MMI06-24-11. Zircons from the populations analyzed are pictured in Figure 2, both before and after air abrasion treatment. Four single zircon grains analyzed from sample MMI06-5-1 produced good quality data with four concordant and overlapping 2σ error ellipses contributing to a best estimate concordia age of 171.44 ±0.39 Ma (Fig 3A) at 95% confidence (2σ decay constant errors included). The mean square of weighted deviates (MSWD) of concordance is 1.3 and the probability of concordance is 0.25.

Three single zircon grains analyzed from sample MMI06-24-11 also produced good-quality data with con-

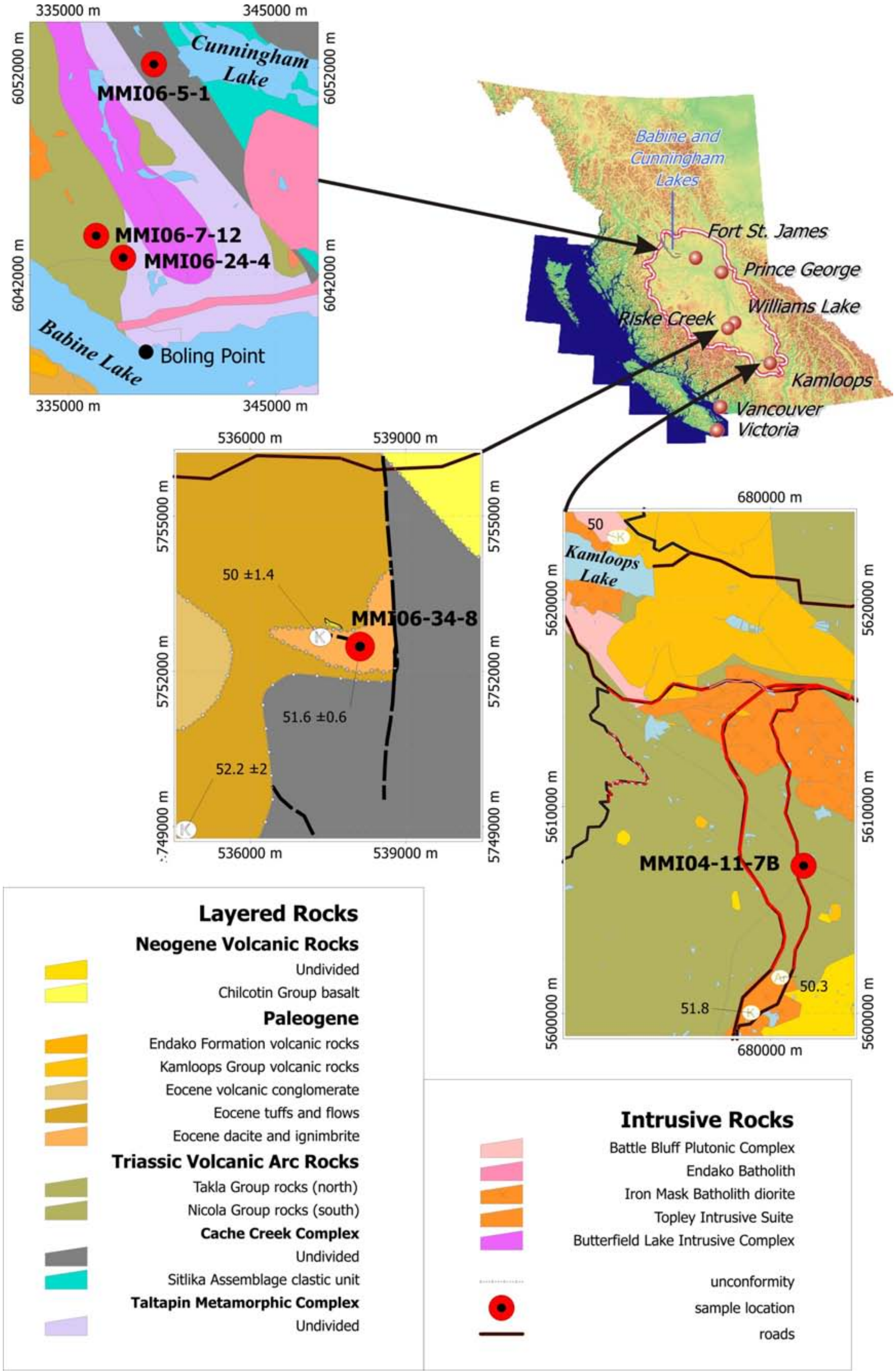

Figure 1. Location of the samples analyzed. Geological maps are modified after Massey et al. (2005) and Mihalynuk and Harker (2007).

TABLE 1. SUMMARY INFORMATION FOR GEOCHRONOLOGICAL SAMPLES.

Sample number	Method and interpreted best age[1]	Location (UTM zone 10)	Lithology sampled	Reason for geochronological age determination
MMI06-5-1	U-Pb zircon 171.4 ±0.4 Ma	339119E, 6052178N; Cunningham Lake	Foliated dacitic ignimbrite	To confirm affiliation of quartz-phyric volcanic unit with the Sitkika assemblage and Kutcho-type volcanogenic massive sulphide potential
MMI06-24-11	U-Pb zircon 218.7 ±0.4 Ma	335309E, 6045571N; Babine Lake	Quartz eye porphyry dike, synkinematic, variable ductile (quartz elongation) fabric	Fabric relationships show that this intrusion was emplaced during deformation; age determination will date the deformation, probably ca. 200 Ma
MMI04-11-7b	$^{40}Ar/^{39}Ar$ muscovite/ whole rock 53.39 ±0.45 Ma	681606E, 5607143N; Iron Mask batholith	Fine-grained muscovite-quartz-carbonate schist	Sample is within the Cherry Creek tectonic zone; age determination will provide a minimum age for this deformation
MMI06-24-4	$^{40}Ar/^{39}Ar$ biotite 134.65 ±0.74 Ma	337638E, 6042831N; Babine Lake	Sparse biotite booklets in porphyritic, intermediate to mafic volcanic breccia, deformed to chlorite-actinolite-epidote schist	Cooling age of metamorphism, which has not previously been dated
MMI06-34-8	$^{40}Ar/^{39}Ar$ hornblende 51.65 ±0.58 Ma	538117E, 5752479N; Riske Creek	Ignimbritic lapilli tuff-breccia composed of acicular hornblende (10%), biotite (1%), quartz eyes (15%) and feldspar (40%, mainly K-feldspar) in a fine-grained, light grey matrix	Cooling age of eruptive unit; K-Ar whole rock age on same package of rocks was reported as 50 ±1.4 Ma (Hunt and Roddick, 1994; MacIntyre et al., 2001)

[1] Precision for all interpreted ages at 95% confidence limit, decay constant errors included.

cordant and overlapping 2σ error ellipses contributing to a best estimate concordia age of 218.74 ±0.44 Ma (Fig 3B) at 95% confidence (2σ decay constant errors included). The MSWD of concordance is 2.0 and the probability of concordance is 0.19.

Argon-40/argon-39 analyses were performed on three samples: MMI04-11-7b (whole rock containing white mica), MMI06-24-4 (biotite) and MMI06-34-8 (hornblende).

Whole rock sample MMI04-11-7b produced a good 53.39 ±0.45 Ma plateau age (2σ, including J-error of 0.5%) representing 82.7% of the ^{39}Ar gas released (Fig 4A). The MSWD of concordance is 0.76 and the probability of concordance is 0.55. The inverse isochron has an initial $^{40}Ar/^{36}Ar$ intercept of 311 ±19 Ma, within error of the accepted atmospheric value, and yielded an age of 52.82 ±0.83 Ma (MSWD = 0.115).

The biotite separate (sample MMI06-24-4) produced a convincing plateau for intermediate heating steps only (Fig 4B). Accounting for 51.7% of the ^{39}Ar gas released, the plateau age is 134.65 ±0.74 Ma (2σ, including J-error of 0.5%). The MSWD of concordance is 1.00 and the probability of concordance is 0.41. The inverse isochron is poorly constrained due to radiogenic argon dominating the heating steps, yielding an initial $^{40}Ar/^{39}Ar$ intercept of 290 ±98 Ma, an age of 134.9 ±4.3 Ma, and a MSWD = 1.3, but nonetheless supports the plateau age.

The hornblende separate (sample MMI06-34-8) produced a 51.65 ±0.58 Ma plateau age (2σ, including J-error of 0.5%) representing 90% of the ^{39}Ar gas released (Fig 4C). The MSWD is 0.49 and the probability of concordance is 0.61. Again, the inverse isochron is dominated by radiogenic argon, yielding a poorly constrained but supportive initial $^{40}Ar/^{36}Ar$ intercept of 275 ±64 Ma and age of 51.8 ±2.1 Ma (MSWD = 0.71).

GEOLOGICAL IMPLICATIONS OF GEOCHRONOLOGICAL RESULTS

Babine Lake

Geological fieldwork was conducted in the southern Babine Lake area as a consequence of province-wide Regional Geochemical Stream sediment compilations that showed correlations between phosphorous and copper (Mihalynuk et al., 2007; cf., Lett et al., 2008). These elements show strong correlation in alkalic copper-gold porphyry camps such as the Iron Mask batholith and Mount Polley. Mineralization at most alkalic copper-gold porphyry deposits within the province is between 205 and 200 Ma (Logan et al., 2007). One objective of the work in the Babine Lake area was to determine if any intrusive rocks of this critical age are present.

BOLING POINT AREA: SYNKINEMATIC DIKE, SAMPLE MMI06-24-11

Between approximately 1 km and 7 km northwest of Boling Point on Babine Lake (Fig 1), exposures are dominated by foliated mafic volcanic rocks. These are mainly coarse-grained pyroxene-porphyritic breccias in which

TABLE 2. U-PB TIMS ANALYTICAL DATA FOR ZIRCON.

Fraction[1]	Weight (µg)	U^2 (ppm)	Pb^3 (ppm)	$^{206}Pb/^{204}Pb^4$	Pb^5 (pg)	Th/U^6	Isotopic ratios ±1σ(%)[7] $^{206}Pb/^{238}U$	$^{207}Pb/^{235}U$	$^{206}Pb/^{206}Pb$	ρ[8]	%[9] discordant	Apparent ages ±2σ (Ma)[7] $^{206}Pb/^{238}U$	$^{207}Pb/^{235}U$	$^{206}Pb/^{206}Pb$
Sample MMI06-5-1														
A	10	294.65	8.20	2639	1.9	0.468	0.02698 ±0.10	0.1843 ±0.25	0.04955 ±0.22	0.47733	1.5	171.6 ±0.4	171.8 ±0.8	174.1 ±10.4/10.4
B	7	293.07	8.10	1604	2.2	0.426	0.02699 ±0.11	0.1840 ±0.36	0.04945 ±0.33	0.39715	–1.5	171.7 ±0.4	171.5 ±1.1	169.1 ±15.2/15.4
C	11	237.42	6.70	2712	1.6	0.547	0.02692 ±0.08	0.1854 ±0.45	0.04995 ±0.42	0.47712	11.3	171.3 ±0.3	172.7 ±1.4	192.8 ±19.5/19.7
D	10	199.10	5.70	1454	2.3	0.566	0.02697 ±0.33	0.1844 ±0.47	0.04959 ±0.49	0.30548	2.5	171.5 ±1.1	171.8 ±1.5	175.9 ±22.5/22.8
Sample MMI06-24-11														
C	11	184.71	6.20	218.2	21.6	0.275	0.03443 ±0.27	0.23994 ±1.17	0.05054 ±1.02	0.637034	0.8	218.2 ±1.2	218.4 ±4.6	220.0 ±46.4/47.7
D	13	174.11	6.00	1216	4.0	0.317	0.03453 ±0.10	0.23949 ±0.27	0.05031 ±0.23	0.515749	–4.6	218.8 ±0.4	218.0 ±1.0	209.3 ±10.6/10.7
E	8	153.68	5.30	1282	2.1	0.319	0.03456 ±0.23	0.24065 ±0.61	0.05050 ±0.55	0.457242	–0.4	219.0 ±1.0	219.0 ±2.4	218.2 ±25.1/25.5

[1] All grains air abraded; all single grains processed and analyzed, except where noted by number of grains after fraction ID.

[2] U blank correction of 0.2pg ± 20%; U fractionation corrections were measured for each run with a double $^{233\text{-}235}U$ spike.

[3] Radiogenic Pb: all raw Pb data corrected for fractionation of 0.23%/amu ± 20% determined by repeat analysis of NBS-982 reference material.

[4] Measured ratio corrected for spike and Pb fractionation.

[5] Total common Pb in analysis based on blank isotopic composition: $^{206}Pb/^{204}Pb$ = 18.5 ± 3%, $^{207}Pb/^{204}Pb$ = 15.5 ± 3%, $^{208}Pb/^{204}Pb$ = 36.4 ± 0.5%.

[6] Model Th/U derived from radiogenic ^{208}Pb and the $^{207}Pb/^{206}Pb$ age of fraction.

[7] Fractionation, blank and common Pb corrected: Pb procedural blanks were ~2.0 pg and U <0.2 pg. Common Pb compositions are based on Stacey-Kramers (Stacey and Kramers, 1975) model Pb at the interpreted age of the rock — 219 Ma for sample MMI06-24-11 and 172 Ma for sample MMI06-24-11 .

[8] Correlation coefficient.

[9] Discordance in % to origin.

TABLE 3. ^{40}AR/^{39}AR STEP HEATING GAS RELEASE DATA.

Laser power (%)	^{40}Ar/^{39}Ar	^{38}Ar/^{39}Ar	^{37}Ar/^{39}Ar	^{36}Ar/^{39}Ar	Ca/K	Cl/K	%^{40}Ar atm	f ^{39}Ar	^{40}Ar/^{39}ArK	Age
Sample MMI04-11-7b: whole rock white mica, J = 0.010308±0.000012, integrated age = 53.26±0.43 Ma (2σ)										
2	16.155 ±0.012	0.064 ±0.083	0.097 ±0.057	0.049 ±0.037	1.75	0.008	85.21	1.18	2.270 ±0.545	41.74 ±9.91
2.3	4.884 ±0.026	0.027 ±0.045	0.435 ±0.027	0.010 ±0.058	9.218	0.002	46.86	4.94	2.470 ±0.187	45.36 ±3.38
2.4	3.767 ±0.014	0.018 ±0.054	0.627 ±0.019	0.005 ±0.073	13.35	0	19.99	8.37	2.903 ±0.121	53.19 ±2.18
2.7	3.115 ±0.007	0.014 ±0.029	0.099 ±0.020	0.001 ±0.095	2.089	0	4.71	21.18	2.892 ±0.036	53.00 ±0.65
3	3.880 ±0.004	0.013 ±0.039	0.007 ±0.033	0.003 ±0.029	0.126	0	22.92	29.73	2.931 ±0.031	53.70 ±0.56
3.2	3.672 ±0.004	0.014 ±0.029	0.008 ±0.057	0.003 ±0.050	0.139	0	18.45	15.22	2.909 ±0.041	53.30 ±0.75
3.4	3.856 ±0.005	0.014 ±0.056	0.010 ±0.057	0.003 ±0.104	0.165	0	20.46	8.19	2.940 ±0.102	53.87 ±1.84
3.7	3.860 ±0.005	0.015 ±0.044	0.013 ±0.039	0.003 ±0.100	0.236	0	17.17	7.86	3.062 ±0.087	56.06 ±1.56
4	4.729 ±0.006	0.014 ±0.076	0.030 ±0.058	0.006 ±0.075	0.518	-0.001	27.3	3.33	3.199 ±0.131	58.54 ±2.36
Total/average	*3.807 ±0.001*	*0.015 ±0.008*	*1.167 ±0.001*	*0.003 ±0.011*	*2.138*	*0.001*		*100*	*2.907 ±0.012*	
Sample MMI06-24-4: biotite ± hornblende, J = 0.010300±0.000012, integrated age = 136.01±0.31 Ma (2σ)										
2	20.276 ±0.012	0.053 ±0.043	0.036 ±0.075	0.041 ±0.031	0.661	0.007	55.68	0.42	8.556 ± 0.393	152.38 ±6.72
2.2	13.069 ±0.006	0.036 ±0.074	0.031 ±0.055	0.025 ±0.037	0.581	0.004	51.64	0.62	5.981 ± 0.271	107.85 ±4.74
2.4	9.411 ±0.004	0.023 ±0.029	0.022 ±0.023	0.012 ±0.024	0.457	0.002	35.57	3.03	5.942 ± 0.088	107.16 ±1.54
2.7	8.631 ±0.004	0.020 ±0.022	0.019 ±0.026	0.005 ±0.027	0.408	0.001	17.21	5.37	7.045 ± 0.053	126.38 ±0.93
2.9	8.398 ±0.005	0.019 ±0.022	0.025 ±0.017	0.003 ±0.037	0.537	0.001	9.79	7.09	7.486 ± 0.049	134.00 ±0.85
3.1	8.388 ±0.005	0.019 ±0.026	0.038 ±0.014	0.003 ±0.037	0.817	0.001	9.38	8.19	7.517 ± 0.048	134.54 ±0.83
3.3	8.307 ±0.005	0.019 ±0.020	0.072 ±0.014	0.003 ±0.027	1.554	0.001	8.68	11.32	7.517 ± 0.042	134.53 ±0.72
3.4	8.255 ±0.004	0.020 ±0.020	0.102 ±0.017	0.003 ±0.033	2.202	0.001	7.94	7.94	7.518 ± 0.044	134.56 ±0.75
3.5	8.378 ±0.004	0.019 ±0.017	0.089 ±0.015	0.003 ±0.032	1.92	0.001	8.83	7.37	7.553 ± 0.043	135.17 ±0.73
3.6	8.404 ±0.004	0.020 ±0.023	0.097 ±0.014	0.003 ±0.022	2.085	0.001	9.46	9.77	7.537 ± 0.040	134.87 ±0.69
3.7	8.570 ±0.005	0.018 ±0.029	0.082 ±0.018	0.003 ±0.030	1.777	0.001	8.47	8.29	7.763 ± 0.045	138.78 ±0.78
3.8	8.685 ±0.005	0.019 ±0.027	0.092 ±0.017	0.003 ±0.045	1.994	0.001	7.69	6.23	7.923 ± 0.055	141.52 ±0.94
3.9	8.711 ±0.004	0.019 ±0.019	0.112 ±0.015	0.003 ±0.040	2.424	0.001	7.53	5.27	7.951 ± 0.048	142.01 ±0.83
4.1	8.586 ±0.005	0.018 ±0.024	0.072 ±0.016	0.002 ±0.033	1.548	0.001	6.92	7.5	7.905 ± 0.045	141.22 ±0.77
4.3	8.683 ±0.004	0.017 ±0.018	0.051 ±0.018	0.002 ±0.035	1.099	0.001	5.91	5.97	8.069 ± 0.040	144.03 ±0.69
4.6	8.680 ±0.005	0.017 ±0.016	0.077 ±0.015	0.002 ±0.042	1.657	0.001	6.04	5.64	8.053 ±0.048	143.76 ±0.82
Total/average	*8.516 ±0.001*	*0.019 ±0.003*	*0.829 ±0.001*	*0.003 ±0.004*	*1.517*	*0.002*		*100*	*7.522 ± 0.008*	
Sample MMI06-34-8: hornblende, J = 0.010322 ±0.000010, integrated age = 48.86 ±0.69 Ma (2σ)										
2	241.226 ±0.033	0.374 ±0.114	0.688 ±0.071	0.883 ±0.050	8.829	0.05	108.61	0.1	–17.807 ±9.833	–366.40 ±224.33
2.2	78.656 ±0.026	0.187 ±0.177	0.361 ±0.077	0.311 ±0.071	4.971	0.029	119.43	0.22	–12.214 ±6.083	–243.12 ±129.62
2.5	15.918 ±0.012	0.061 ±0.174	0.246 ±0.050	0.056 ±0.082	4.737	0.009	100.72	0.94	–0.118 ±1.339	–2.20 ±24.97
2.8	13.347 ±0.006	0.069 ±0.060	0.074 ±0.040	0.039 ±0.049	1.357	0.011	83.05	2.34	1.984 ±0.563	36.58 ±10.28
3.1	6.864 ±0.008	0.164 ±0.033	0.115 ±0.042	0.018 ±0.055	2.269	0.034	68.77	2.31	1.653 ±0.293	30.52 ±5.37
3.4	5.019 ±0.007	0.378 ±0.017	0.276 ±0.024	0.011 ±0.062	5.949	0.084	50.02	4.09	2.066 ±0.203	38.06 ±3.70
3.7	3.744 ±0.005	0.343 ±0.010	0.356 ±0.014	0.004 ±0.037	7.854	0.076	21.83	22.89	2.785 ±0.051	51.13 ±0.92
4	3.143 ±0.005	0.259 ±0.010	0.366 ±0.013	0.002 ±0.056	8.318	0.057	7.33	40.62	2.809 ±0.042	51.57 ±0.76
4.3	3.313 ±0.005	0.252 ±0.011	0.379 ±0.013	0.003 ±0.069	8.611	0.055	9.35	26.49	2.862 ±0.060	52.52 ±1.08
Total/average	*3.941 ±0.001*	*0.273 ±0.003*	*4.276 ±0.001*	*0.005 ±0.011*	*7.849*	*0.045*		*100*	*2.819 ±0.019*	

Notes:

Gas volume measurements to 10^{-13} cm^3

Neutron flux monitors: 28.02 Ma FCs (Renne et al., 1998)

Isotope production ratios: (^{40}Ar/^{39}Ar)K = 0.0302 ±0.00006, (^{37}Ar/^{39}Ar)Ca = 1416 ±0.5, (^{36}Ar/^{39}Ar)Ca = 0.3952 ±0.0004, Ca/K = 1.83 ±0.01 (^{37}ArCa/^{39}ArK) pyroxene crystals have acted as strain markers and display flattening and orogen-parallel elongation within the foliation planes. Elongation strain averages about 3 but can exceed 10 (Fig 5). Foliation and lineation fabrics are cut by a granodioritic pluton 6 km in length and by smaller stocks less than a kilometre in length (MacIntyre and Schiarizza, 1999). All are elongated in a northwest direction, parallel with the mineral elongation direction which averages approximately 335°.

Hornblende dacite dikes generally cut the foliation of the deformed volcanic country rocks (Fig 6). The dikes are 1 to 5 m thick and have an average strike/dip of approximately 145°/60°. They all display protomylonitic textures. Locally, the dikes are transposed by the 335° ductile fabric. These relationships are taken to indicate late synkinematic emplacement of the dikes.

The U-Pb zircon age determination of 218.7 ±0.4 Ma for sample MMI06-24-11, collected from one of the synkinematic dacite dikes, is slightly younger than the crystallization age of 226 ±3 Ma estimated from a stock 2 km to the southeast by MacIntyre et al. (2001). This stock displays a decimetre thick ultramylonite zone (approx. 205°/40°) that is overprinted by later dilational brecciation textures (Fig 7).

The new age is identical, within the limits of error, to the oldest parts of the Endako Batholith (the Stern Creek phase) where dated, approximately 65 km to the southeast.

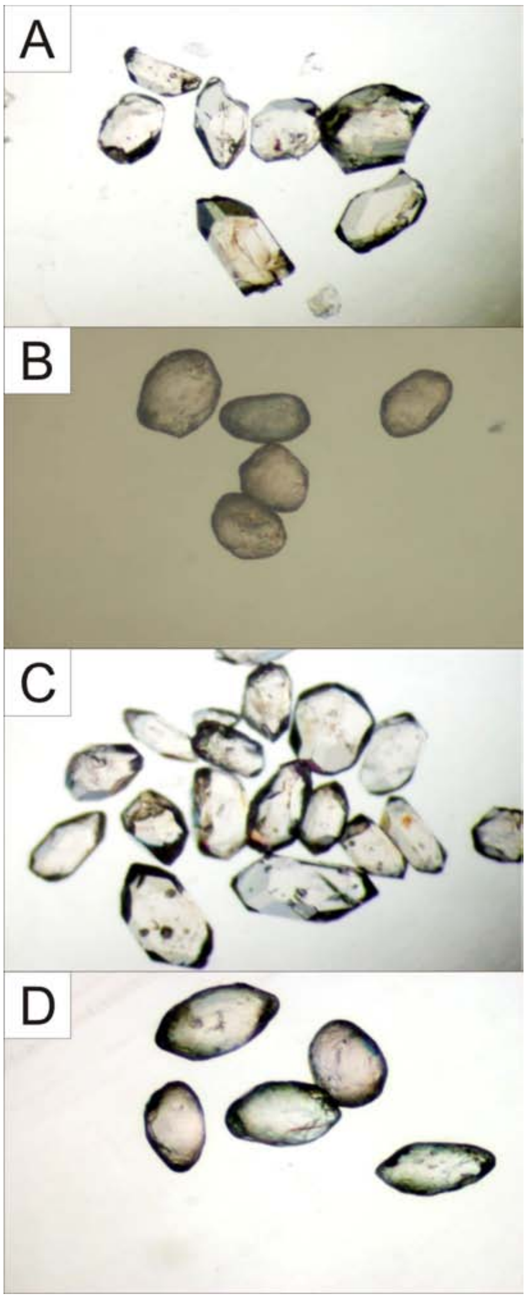

Figure 2. Photomicrographs of zircons analyzed from sample MMI06-5-1 before (A) and after (B) air abrasion, and from sample MMI06-24-11 before (C) and after (D) air abrasion. Horizontal dimension of photos represents approximately 1 mm.

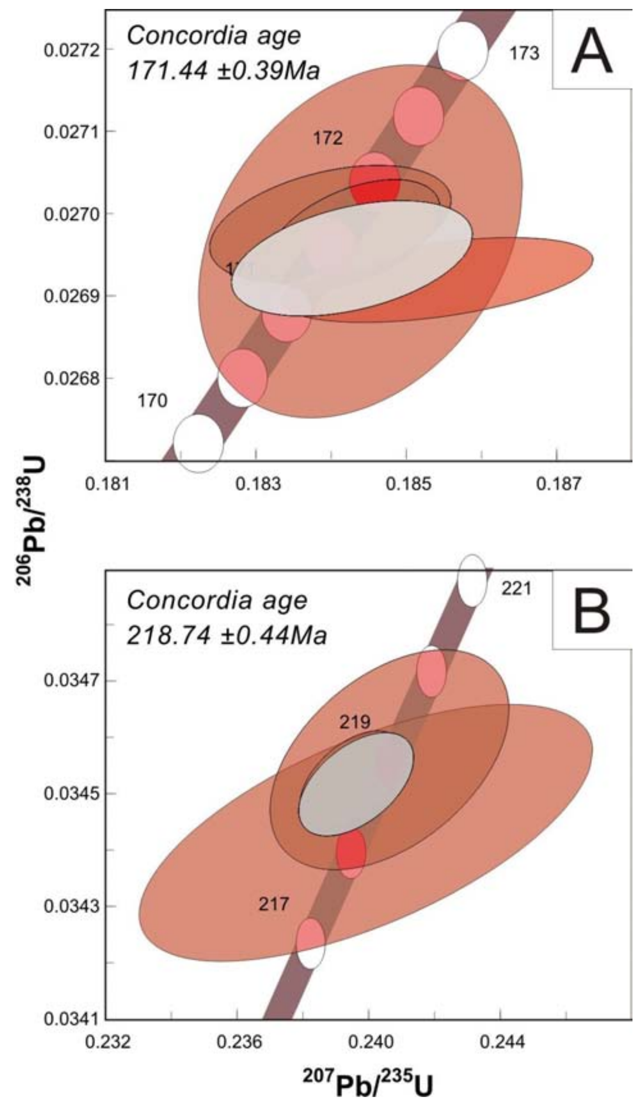

Figure 3. Concordia plots for U-Pb TIMS data for: A) sample MMI06-5-1, and (B) sample MMI06-24-11. 2σ error ellipses for individual analytical fractions are shown in red. These data are combined to produce the best estimate age shown by the grey ellipse. Concordia bands include 2σ errors on U decay constants.

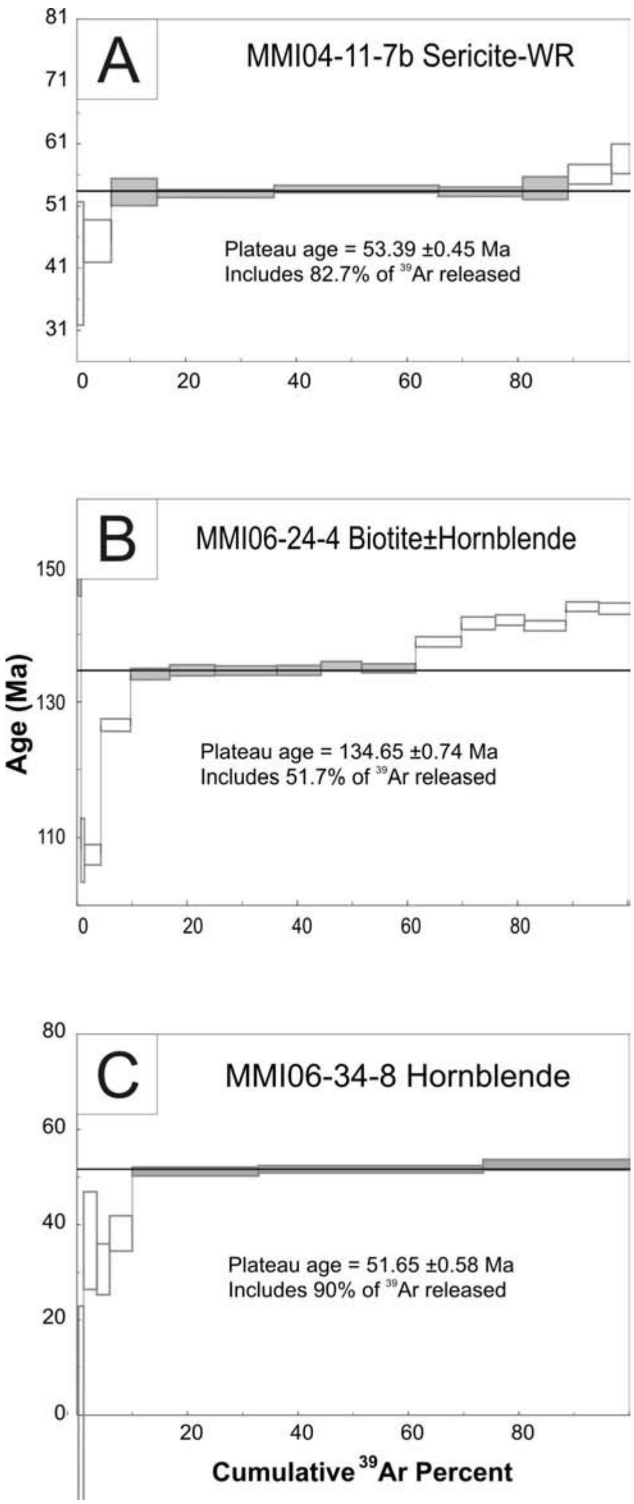

Figure 4. Step heating Ar gas release spectra for: A) sample MMI04-11-7b, B) sample MMI06-24-4, and C) sample MMI06-34-8. Plateau steps are filled, rejected steps are open. Box heights at each step are 2σ.

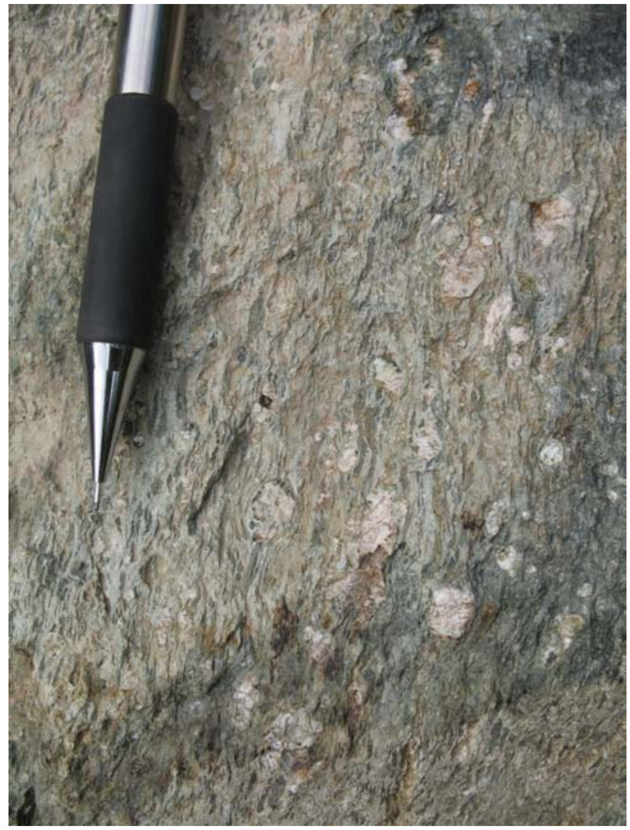

Figure 5. Coarse augite crystals characterize the porphyritic volcanic rocks near Boling Point. They are good strain markers and commonly display a strong lineation. Strain averages about 3, but is locally 10 or more.

Figure 6. Dacite dike contact shows weakly to non-foliated dike margin in contact with foliated tuffaceous country rocks.

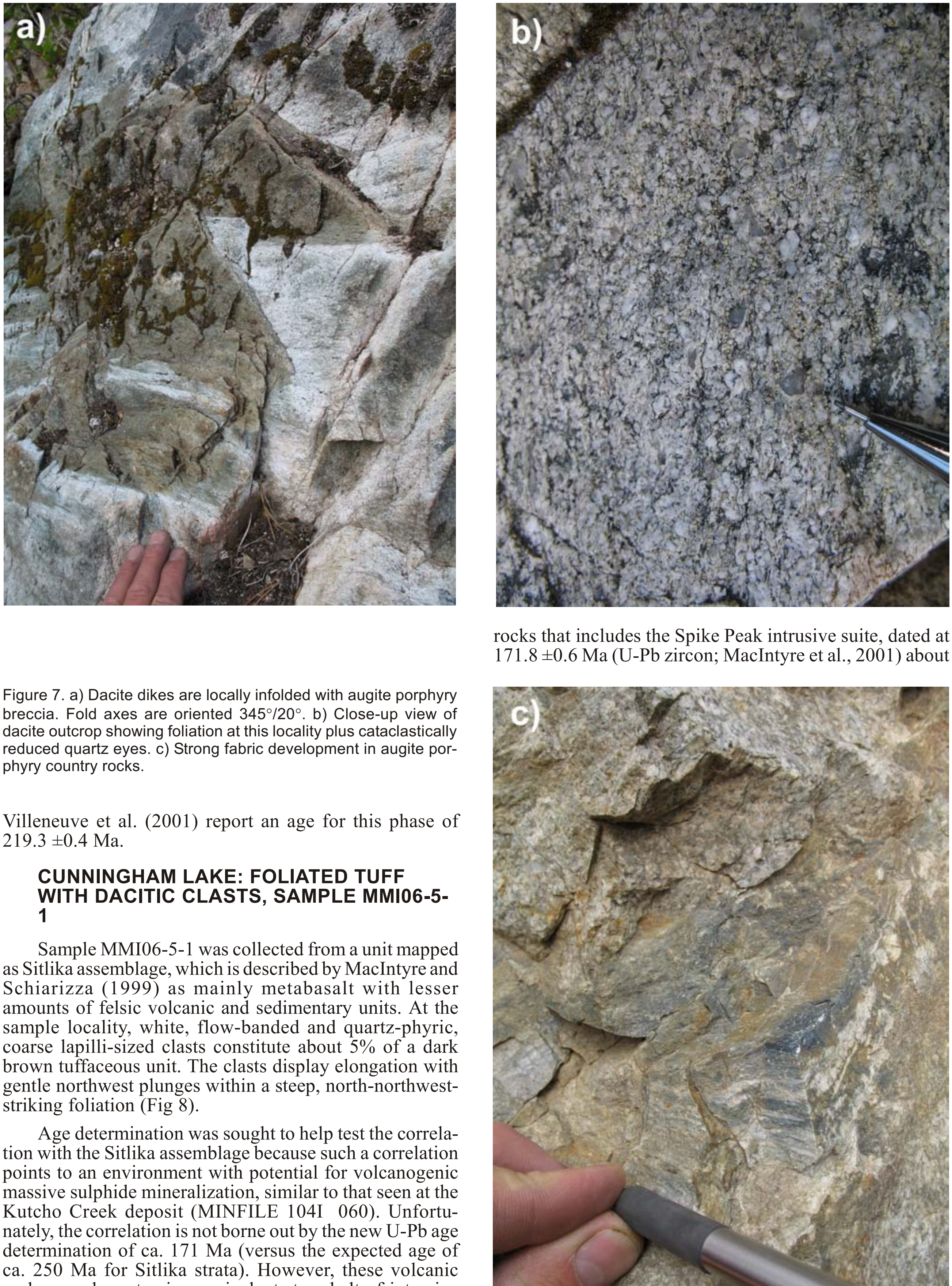

Figure 7. a) Dacite dikes are locally infolded with augite porphyry breccia. Fold axes are oriented 345°/20°. b) Close-up view of dacite outcrop showing foliation at this locality plus cataclastically reduced quartz eyes. c) Strong fabric development in augite porphyry country rocks.

Villeneuve et al. (2001) report an age for this phase of 219.3 ±0.4 Ma.

CUNNINGHAM LAKE: FOLIATED TUFF WITH DACITIC CLASTS, SAMPLE MMI06-5-1

Sample MMI06-5-1 was collected from a unit mapped as Sitlika assemblage, which is described by MacIntyre and Schiarizza (1999) as mainly metabasalt with lesser amounts of felsic volcanic and sedimentary units. At the sample locality, white, flow-banded and quartz-phyric, coarse lapilli-sized clasts constitute about 5% of a dark brown tuffaceous unit. The clasts display elongation with gentle northwest plunges within a steep, north-northwest-striking foliation (Fig 8).

Age determination was sought to help test the correlation with the Sitlika assemblage because such a correlation points to an environment with potential for volcanogenic massive sulphide mineralization, similar to that seen at the Kutcho Creek deposit (MINFILE 104I 060). Unfortunately, the correlation is not borne out by the new U-Pb age determination of ca. 171 Ma (versus the expected age of ca. 250 Ma for Sitlika strata). However, these volcanic rocks may be extrusive equivalents to a belt of intrusive rocks that includes the Spike Peak intrusive suite, dated at 171.8 ±0.6 Ma (U-Pb zircon; MacIntyre et al., 2001) about

75 km along strike to the northwest and the Sugarloaf phase of the Endako Batholith, dated at 171 ±1.7 Ma ($^{40}Ar/^{39}Ar$; Villeneuve et al., 2001) about 90 km to the southeast. The deformation event that produced the strong lineation displayed by these pyroclastic strata must be younger than ca. 171 Ma.

BOLING POINT: BIOTITE GRADE METATUFF, SAMPLE MMI06-24-4

Late Triassic augite porphyritic volcanic and related sedimentary rocks are in presumed contact with serpentinized ultramafic rocks along their eastern margin (MacIntyre and Schiarizza, 1999) in the Boling Point area, but the contact is obscured by surficial deposits. At the sample locality, augite porphyry breccia contains sparse, possibly andesitic, clasts containing euhedral biotite booklets. Biotite was extracted from one of these clasts for geochronological age determination and yielded a cooling age of 134.65 ±0.74 Ma (Table 3).

Elongation fabrics at the sample locality are similar to other parts of the Late Triassic package near Boling Point and the Middle Jurassic section at Cunningham Lake. To the immediate east, however, polydeformed, fine-grained tuffaceous sedimentary rocks may have been deformed into sheath folds (Fig 9). In consideration of the protolith age of the sample from Cunningham Lake (ca. 171 Ma), the strong metamorphic fabric was probably imparted on this belt of rocks between ca. 171 and ca. 135 Ma.

Riske Creek area

Two K-Ar whole rock ages are reported from unnamed Eocene volcanic rocks in the Riske Creek area. They are 52.2 ±2 Ma and 50 ±1.4 Ma (Hunt and Roddick, 1994). A clean fresh sample of hornblende-porphyritic tuff was collected to obtain a more robust $^{40}Ar/^{39}Ar$ age. The aim was to test the chronostratigraphic correlation of these rocks with lithologically similar rocks more than 100 km to the west-northwest, now the subject of geological investigation (Mihalynuk et al., 2008), and a growing body of radiometric age data that points to a voluminous ca. 52 Ma eruptive epoch (Riddell et al., 2007).

RISKE CREEK: IGNIMBRITIC TUFF, SAMPLE MMI06-34-8

Slabby-weathering, cream-coloured dacitic ignimbrite cooling units are stacked more than 100 m thick near the sample site. Lahar layers up to 5 m thick locally separate the dacite flows. Lapilli compaction and flow fabrics dip shallowly east-northeast, defined partly by the alignment of oxyhornblende (10%) and biotite (1%, not present in dated sample), together with trails of feldspar (40%) and quartz (15%), in a fine-grained, cream-coloured matrix. These rocks are juxtaposed across a steeply dipping, north-trending fault with Paleozoic chert and argillite of the Cache Creek complex (Mihalynuk and Harker, 2007).

Hornblende separated from a sample of the freshest and densest dacite yielded a $^{40}Ar/^{39}Ar$ age of 51.65 ±0.58 Ma. Previously reported K-Ar age determina-

Figure 8. Lineation of felsic clasts within exposures near Cunningham Lake.

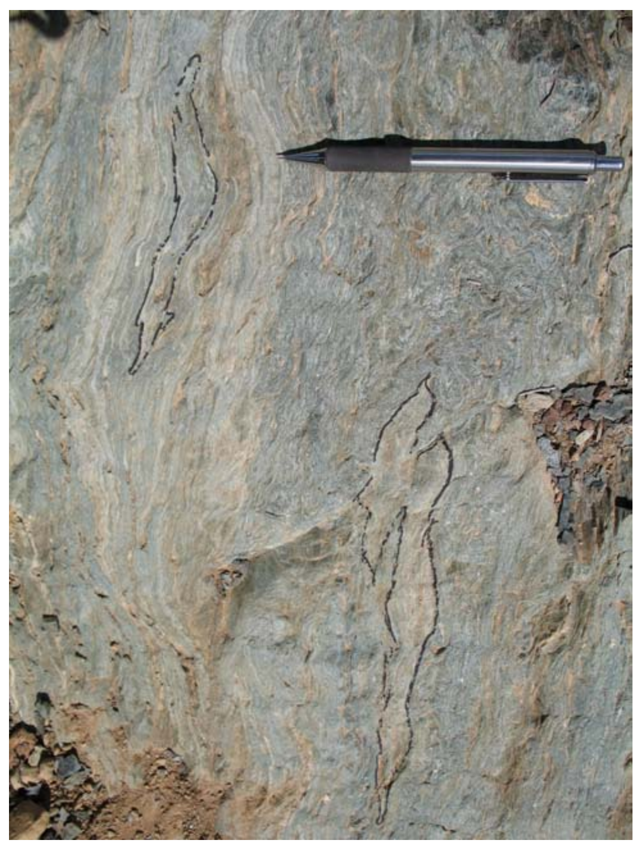

Figure 9. Possible sheath folds within epidote-chlorite-altered tuffaceous siltstone and fine-grained sandstone are outlined in black marker.

tions (Hunt and Roddick, 1994) were from samples of basaltic andesite and dacite tuff collected approximately 0.75 km west and approximately 5 km southwest of sample site MMI06-34-8. The dacite tuff sampled and reported on by Hunt and Roddick (1994) is likely the same unit that is reported on here. The two ages are identical within limits of error. The rocks are equivalent in age to the Ootsa Lake Group to the northwest and the Kamloops Group to the southeast.

Iron Mask batholith

The Iron Mask batholith is an important copper-gold resource as it contains at least eight separate alkalic, porphyry-style copper-gold-silver deposits; five of which are significant past producers. Phyllitic fabrics and minor folds are locally developed in parts of the batholith (Logan et al., 2007). Fabrics with similar orientation are well developed within the Late Triassic arc strata outside the western margin of the batholith. This deformation could affect the distribution of mineralization within the batholith; therefore, it is important to understand its timing as a first step to determining the cause of the deformation.

CHERRY CREEK TECTONIC ZONE PHYLLITE, SAMPLE MMI04-11-7B

In the most coarsely crystalline samples of the phyllite unit, individual mica crystals can be discerned in hand sample. A sample of this calcareous quartz-mica schist was collected from a low, white-weathering outcrop approximately 2 km south of Jacko Lake. Unfortunately, the sample was not sufficiently coarse-grained to permit separation of white mica, so a whole rock determination was performed. It yielded an Eocene $^{40}Ar/^{39}Ar$ age of 53.39 ±0.45 Ma.

Numerous samples collected from within 20 km north and south of Jacko Lake display early Tertiary cooling ages (Matthews, 1964; Preto et al., 1979; Breitsprecher and Mortensen, 2004), but none are from the Mesozoic volcanic section. Two cooling ages for samples of porphyritic granodiorite of the Nicola batholith (Preto et al., 1979) collected from sites approximately 6 and 8 km to the south-southeast of sample site MMI04-11-7b were interpreted on later compilations as having a crystallization age of Late Triassic–Early Jurassic (Kwong, 1987; Massey et al., 2005). The ages are 50.3 ±0.4 Ma ($^{40}Ar/^{39}Ar$, Ghosh, 2003) and 51.8 ±2 Ma (K-Ar, Preto et al., 1979). Volcanic strata of the Kamloops Group, sampled approximately 18 km to the north (approx. 1 km north of Kamloops Lake, Fig 1), have produced a cooling age of 50 ±4 Ma (Matthews, 1964). This sample site is within 100 m of an Eocene pluton that is part of the Battle Bluff plutonic complex (Massey et al., 2005), and the age may partly reflect cooling of that body.

Ductile Eocene deformation may be related to emplacement of an Eocene component of the Nicola batholith, recognized by Preto et al. (1979) but not represented in subsequent compilations. Deformation of this age has not been widely acknowledged in this region. Such deformation may have significant implications for mineral exploration, particularly as deeper structural levels of the Iron Mask batholith are targeted.

ACKNOWLEDGMENTS

Assistance with U-Pb geochronology was provided by H. Lin (mineral separations and support with mass spectrometry) and R. Lishansky (grain selection, abrasion and cleanlab work). Sample MMI04-11-7B was collected as part of the Alkalic Copper-Gold Porphyry project, under the sage leadership of James Logan. C. Peat painstakingly created Figure 1.

REFERENCES

Breitsprecher, K. and Mortensen, J.K. (2004): BCAge 2004A - a database of isotopic age determinations for rock units from British Columbia. *BC Ministry of Energy and Mines*, Open File 2004-3 (Release 2.0), 7766 records, 9.3 Mb, URL <http://www.em.gov.bc.ca/Mining/Geolsurv/Publications/OpenFiles/OF2004-03/toc.htm> [December, 2007].

Ghosh, S. (2003): Petrology, geochemistry, geochronology and tectonic history of the Nicola Horst, B.C.; M.Sc. thesis, *Simon Fraser University*, Vancouver, 155 pages.

Hunt, P.A. and Roddick, J.C. (1994): A compilation of K-Ar and ^{40}Ar-^{39}Ar ages: Report 24; *in* Radiogenic Age and Isotopic Studies, Report 8, *Geological Survey of Canada*, Paper 1994-F, pages 125–155.

Kwong, Y.T.J. (1987): Evolution of the Iron Mask batholith and its associated copper mineralization, *BC Ministry of Energy, Mines and Petroleum Resources*, Bulletin 77, includes 1:50 000 scale map, 56 pages.

Lett, R.E., Man, E.C. and Mihalynuk, M.G. (2008): Towards a drainage geochemical atlas for British Columbia; *in* Geological Fieldwork 2007, *BC Ministry of Energy, Mines and Petroleum Resources*, Paper 2008-1, pages 61–68.

Logan, J.M. and Mihalynuk, M.G. (2006): Geology of the Iron Mask batholith, southern British Columbia (NTS 092I/9, 10), *BC Ministry of Energy, Mines and Petroleum Resources*, Open File 2006-11, 1:25 000 scale, URL <http://www.em.gov.bc.ca/Mining/Geolsurv/Publications/OpenFiles/OF2006-11/toc.htm> [November, 2007].

Logan, J.M., Mihalynuk, M.G., Ullrich, T. and Friedman, R.M. (2007): U-Pb ages of intrusive rocks and $^{40}Ar/^{39}Ar$ plateau ages of copper-gold-silver mineralization associated with alkaline intrusive centres at Mount Polley and the Iron Mask batholith, southern and central British Columbia; *in* Geological Fieldwork 2006, *BC Ministry of Energy, Mines and Petroleum Resources*, Paper 2007-1, pages 93–116, URL <http://www.em.gov.bc.ca/DL/GSBPubs/GeoFldWk/2006/11-Logan.pdf> [November, 2007].

MacIntyre, D.G. and Schiarizza, P. (1999): Bedrock geology, Cunningham Lake area (NTS 93K/11, 12, 13, 14), *BC Ministry of Energy, Mines and Petroleum Resources*, Open File 1999-11, 1:100 000 scale.

MacIntyre, D.G., Villeneuve, M.E. and Schiarizza, P. (2001): Timing and tectonic setting of Stikine Terrane magmatism, Babine-Takla lakes area, central British Columbia; *Canadian Journal of Earth Sciences*, Volume 38, pages 579–601.

Massey, N.W.D., MacIntyre, D.G., Desjardins, P.J. and Cooney, R.T. (2005): Digital Geology Map of British Columbia: Whole Province, *BC Ministry of Energy and Mines*, GeoFile 2005-1, 1:250 000 scale, URL <http://www.em.gov.bc.ca/Mining/Geolsurv/Publications/GeoFiles/Gf2005-1/toc.htm> [November 2007].

Matthews, W.H. (1964): Potassium-argon age determinations of Cenozoic volcanic rocks from British Columbia; *Geological Society of America*, Bulletin, Volume 75, pages 465–468.

Mihalynuk, M.G. (2007a): Evaluation of mineral inventories and mineral exploration deficit of the Interior Plateau Beetle Infested Zone (BIZ); *in* Geological Fieldwork 2006, *BC Ministry of Energy, Mines and Petroleum Resources*, Paper 2007-1, pages 137–142, URL <http://www.em.gov.bc.ca/DL/GSBPubs/GeoFldWk/2006/14-Mihalynuk.pdf> [November 2007].

Mihalynuk, M.G. (2007b): Neogene and Quaternary Chilcotin Group cover rocks in the Interior Plateau, south-central British Columbia: A preliminary 3-D thickness model; *in* Geological Fieldwork, *BC Ministry of Energy, Mines and Petroleum Resources*, Paper 2007-1, pages 143–147, URL <http://www.em.gov.bc.ca/DL/GSBPubs/GeoFldWk/2006/15-Mihalynuk.pdf> [November 2007].

Mihalynuk, M.G. and Harker, L.L. (2007): Riske Creek geology (NTS 92O/16W), *BC Ministry of Energy, Mines and Petroleum Resources*, Open File 2007-6, 1:50,000 scale, URL <http://www.em.gov.bc.ca/DL/GSBPubs/OF/2007-6/OF2007-6-RiskeCk-Mihalynuk-Harker.pdf> [November 2007].

Mihalynuk, M.G., Harker, L.L., Lett, R. and Grant, B. (2007): Results of reconnaissance surveys in the Interior Plateau Beetle Infested Zone (BIZ); *BC Ministry of Energy, Mines and Petroleum Resources*, GeoFile 2007-5, URL <http://www.em.gov.bc.ca/Mining/Geolsurv/Publications/GeoFiles/Gf2007-5/toc.htm> [November 2007].

Mihalynuk, M.G., Peat, C.R., Terhune, K. and Orovan, E.A. (2008): Regional geology and resource potential of the Chezacut map area, central British Columbia (NTS 093C/08); *in* Geological Fieldwork 2007, *BC Ministry of Energy, Mines and Petroleum Resources*, Paper 2008-1, pages 117–134.

MINFILE (2007): MINFILE BC mineral deposits database; *BC Ministry of Energy, Mines and Petroleum Resources*, URL <http://www.em.gov.bc.ca/Mining/Geolsurv/Minfile/> [November 2007].

Preto, V.A., Osatenko, M.J., McMillan, W.J. and Armstrong, R.L. (1979): Isotopic dates and strontium isotopic ratios for plutonic and volcanic rocks in the Quesnel Trough and Nicola Belt, south-central British Columbia; *Canadian Journal of Earth Sciences*, Volume 16, pages 1658–1672.

Riddell, J.M., Ferri, F., Sweet, A.R. and O'Sullivan, P.B. (2007): New geoscience data from the Nechako Basin project; *in* The Nechako Initiative – Geoscience Update 2007, *BC Ministry of Energy, Mines and Petroleum Resources*, pages 59–98, URL <http://www.em.gov.bc.ca/dl/OilGas/COG/Nechako_Sheet3.pdf> [November 2007].

Ullrich, T., Friedman, R.M., Mihalynuk, M.G. and Logan, J.M. (2008): Results of field investigations in the Beetle Infested Zone 2006: radiometric age determination data; *BC Ministry of Energy, Mines and Petroleum Resources*, GeoFile 2008-3.

Villeneuve, M.E., Whalen, J.B., Anderson, R.G. and Struik, L.C. (2001): The Endako batholith: episodic plutonism culminating in formation of the Endako porphyry molybdenite deposit, north-central British Columbia; *Economic Geology*, Volume 96, pages 171–196.